Electronic Supplementary Material (ESI) for Journal of Materials Chemistry C.

Reversible Controlled Morphologies Switching between Porous Microspheres and Urchin-like Microcrystals for NaDC/RHB Self-Assembly and Their Multifunctional Applications

Zhaohua Song, Xia Xin*, Jinglin Shen, Han Zhang, Shubin Wang, Yanzhao Yang *

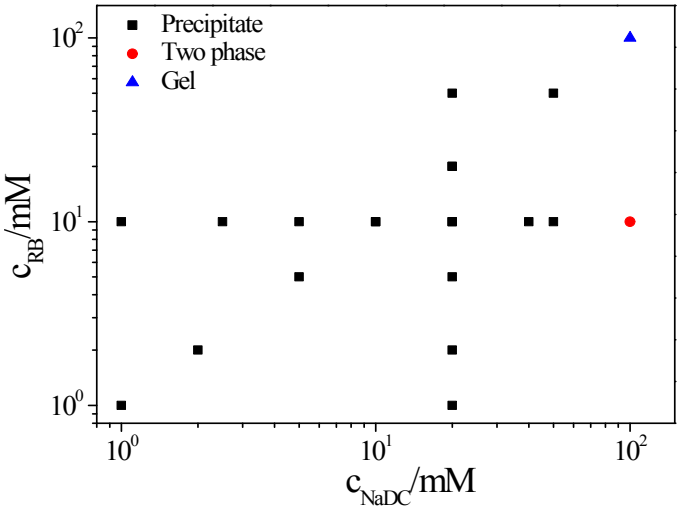

Figure S1 The phase behavior of NaDC/RhB mixed system.

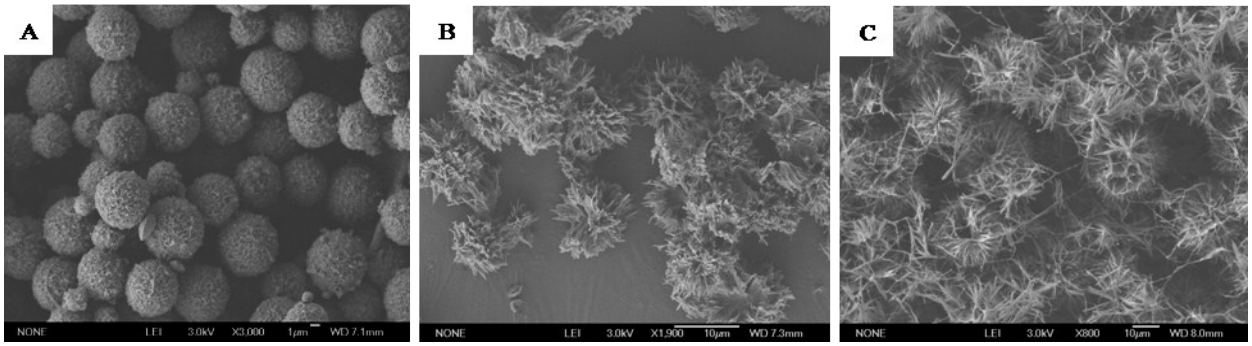

Figure S2 SEM image of the morphologies of precipitate of NaDC/RhB systems: (A) 10 mmol L^{-1} NaDC/10 mmol L^{-1} RhB; (B) 20 mmol L^{-1} NaDC/10 mmol L^{-1} RhB; (C) 50 mmol L^{-1} NaDC/10 mmol L^{-1} RhB.

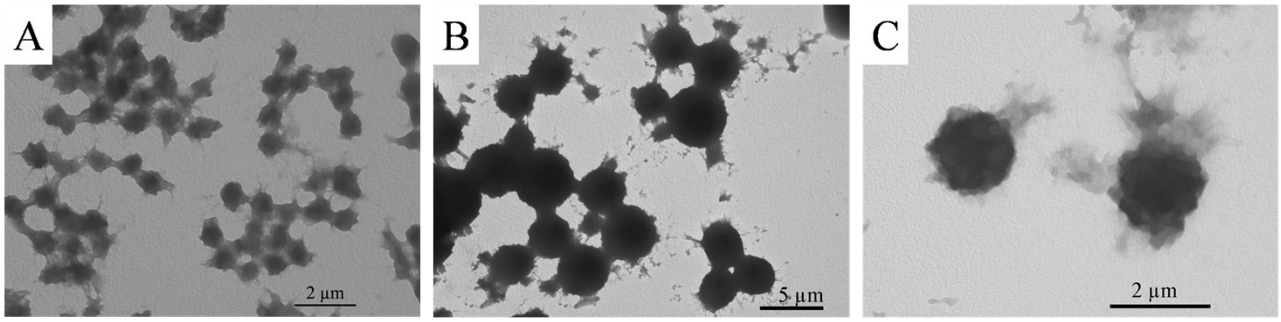

Figure S3 TEM images of NaDC/RhB system when the ratio of NaDC and RhB was fixed at 1:1 (A: 5 mmol L^{-1} NaDC/5 mmol L^{-1} RhB (0.7~1 μm); B: 10 mmol L^{-1} NaDC/10 mmol L^{-1} RhB (3.5-4.5 μm); C: 20 mmol L^{-1} NaDC/20 mmol L^{-1} RhB (2-2.5 μm)).

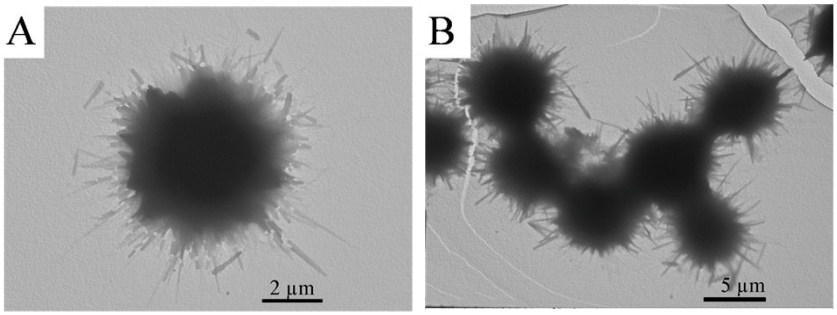

Figure S4 TEM images of NaDC/RhB system when the ratio of NaDC and RhB was fixed at 2:1 (A: 10 mmol L^{-1} NaDC/5 mmol L^{-1} RhB (7~7.5 μm); B: 20 mmol L^{-1} NaDC/10 mmol L^{-1} RhB (6-10.5 μm)).

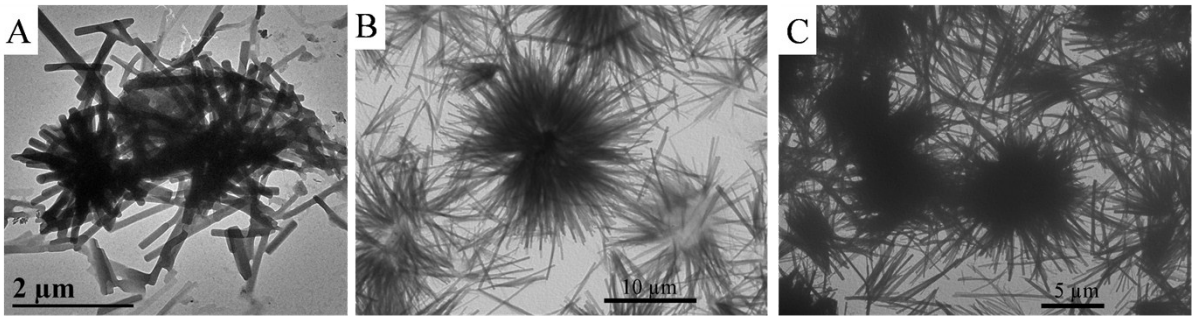

Figure S5 TEM images of NaDC/RhB system when the ratio of NaDC and RhB was fixed at 5:1 (A: 5 mmol L^{-1} NaDC/1 mmol L^{-1} RHB (3.7~5.7 μm); B: 20 mmol L^{-1} NaDC/4 mmol L^{-1} RhB (13.5-15.7 μm); C: 50 mmol L^{-1} NaDC/10 mmol L^{-1} RhB (20.5-23.6 μm)).

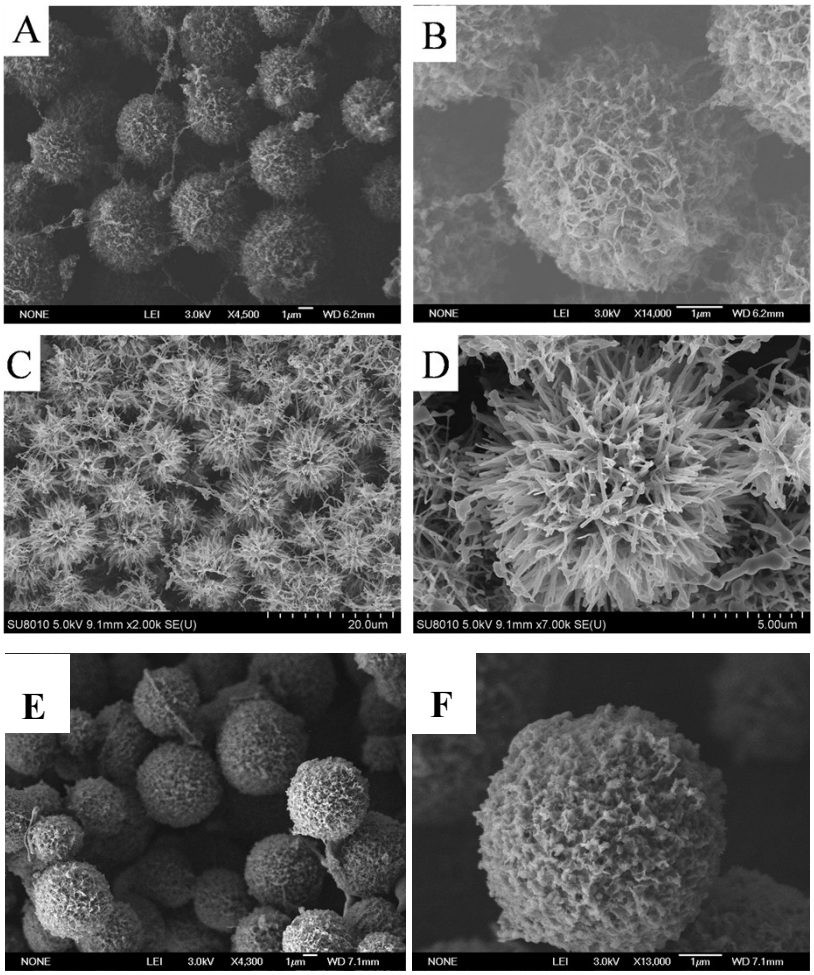

Figure S6 SEM image of the morphologies of precipitate before (A, B) and after (C, D) the addition of 40 mmol L^{-1} NaDC and then (E, F) 40 mmol L^{-1} RhB to 10 mmol L^{-1} NaDC/10 mmol L^{-1} RhB system. The final concentration of NaDC and RhB is 50 mmol L^{-1} NaDC/50 mmol L^{-1} RhB.

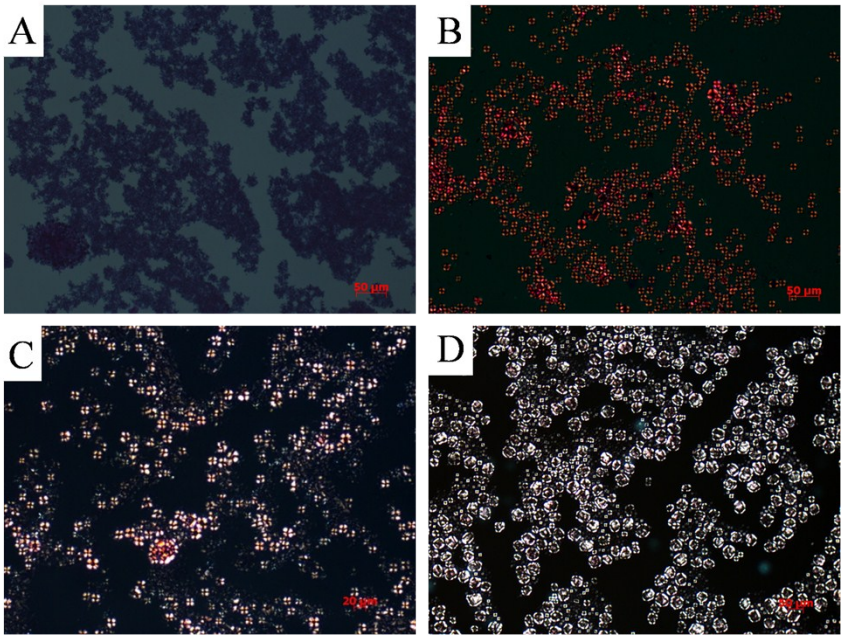

Figure S7 POM image of the precipitates of NaDC/RhB systems: (A) 10 mmol L^{-1} NaDC/10 mmol L^{-1} RhB; (B) 20 mmol L^{-1} NaDC/10 mmol L^{-1} RhB; (C) 50 mmol L^{-1} NaDC/10 mmol L^{-1} RhB; (D) 50 mmol L^{-1} NaDC/10 mmol L^{-1} RhB/NaOH.

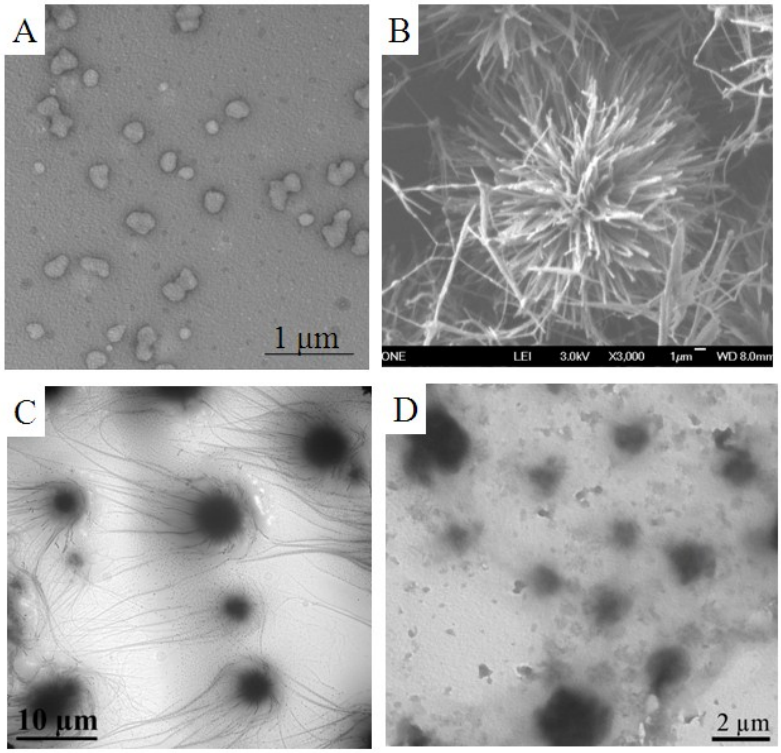

Figure S8 The morphologies of precipitates of 50 mmol L^{-1} NaDC/10 mmol L^{-1} RhB when the pH of the systems were pH = 12 (A); 7.8 (B); 7.2 (C); 6.7 (D).

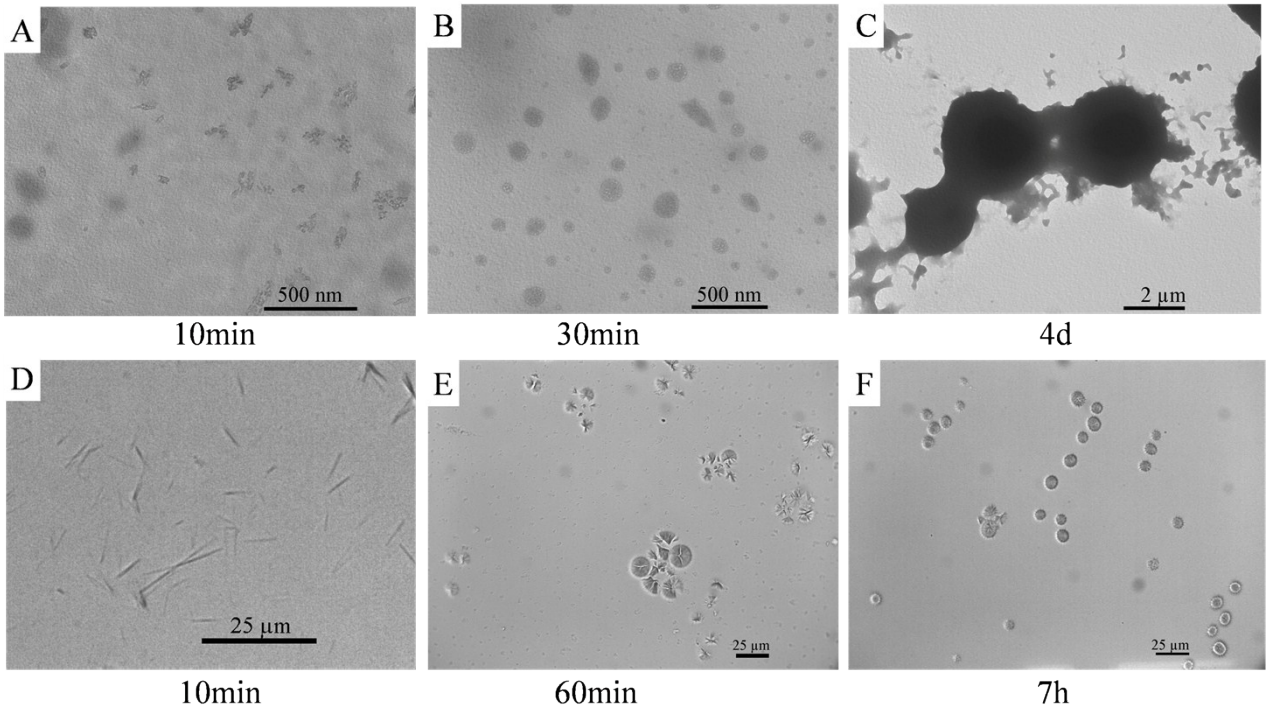

Figure S9 The variation of the morphologies with the aging time for the samples of 10 mmol L^{-1} NaDC/10 mmol L^{-1} RhB(A,B,C) and 50 mmol L^{-1} NaDC/10 mmol L^{-1} RhB(D, E, F).

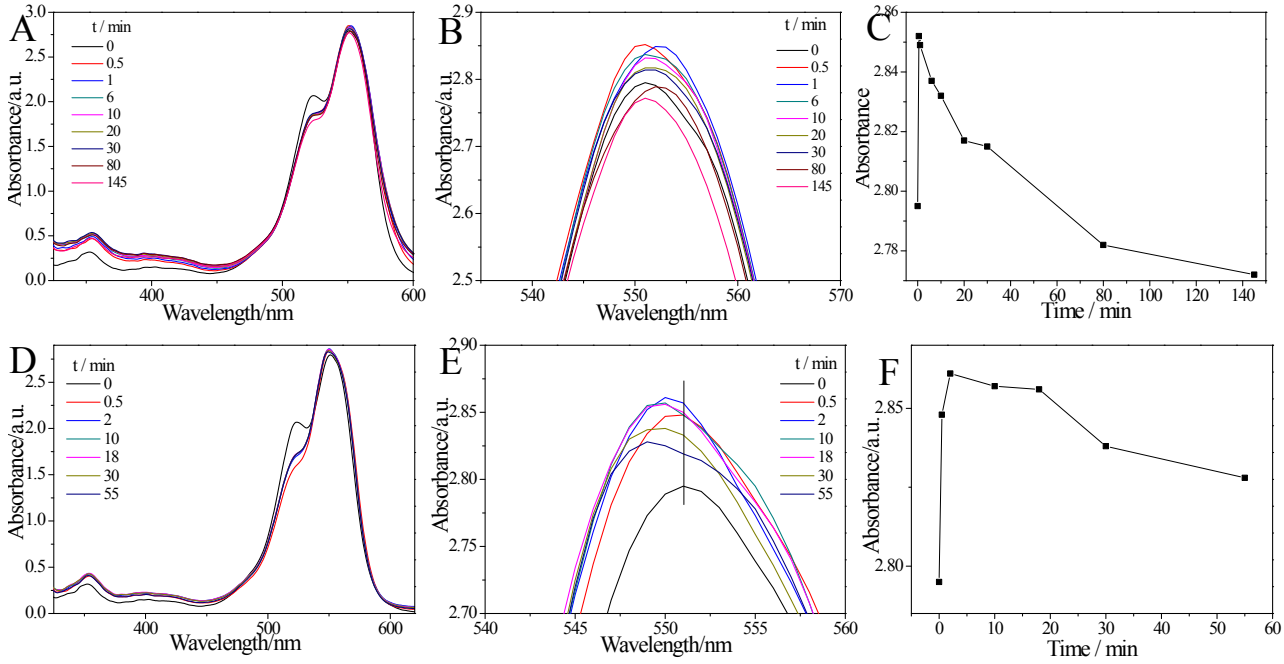

Figure S10 The UV/Vis spectroscopy on time-dependent of the formation of samples of 10 mmol L-1 NaDC/ 10 mmol L-1 RhB (A, B) and 50 mmol L-1 NaDC/ 10 mmol L-1 RhB (D, E) by changes in

the intensities of typical absorption peaks at about 551 nm. (C, F) Plot of maximum absorption intensity at about 551 nm versus time.

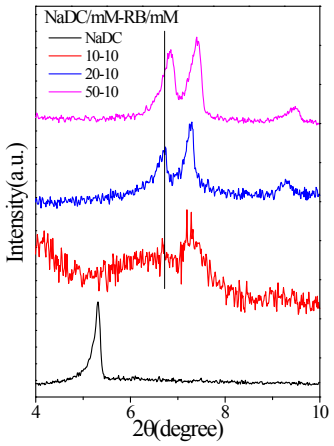

Figure S11 XRD patterns of the NaDC powder and co-assembled structures of NaDC and RhB at a small angle with 2θ from 4° to 10°.

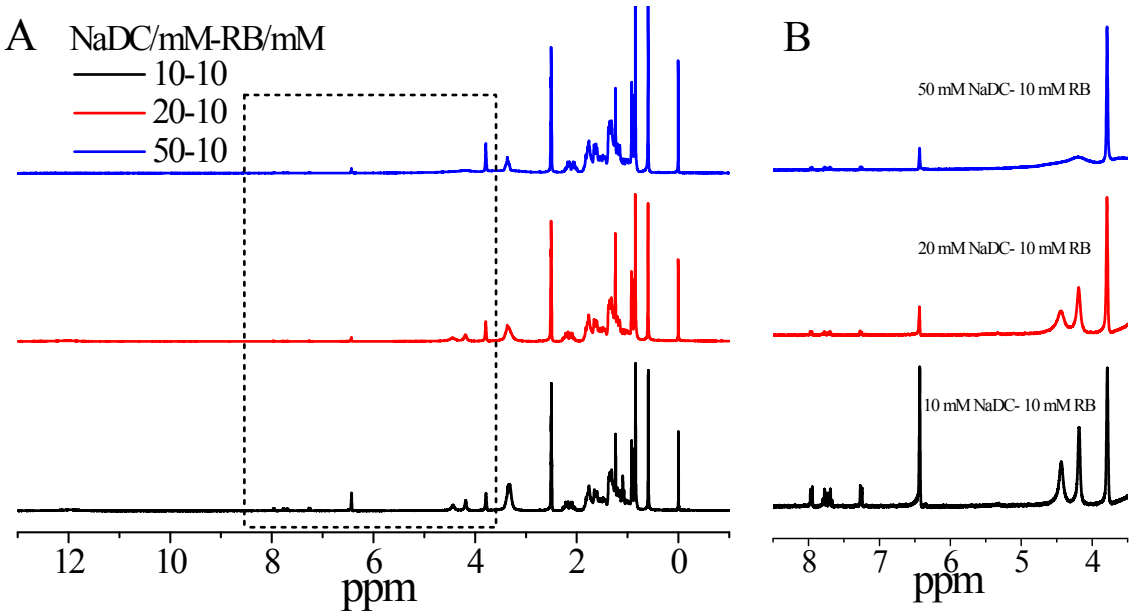

Figure S12 (A): ^{1}HNMR spectrum of NaDC-RhB complexes in [D6]DMSO. (B) is the enlarged part of dashed box of (A).

^{1}HNMR (300 MHz, DMSO-d6, ppm): 0.59 (s, 3H, CH3), 0.84 (s, 3H, CH3), 0.90–0.92 (d, 3H, CH3), 1.0–1.85 (m, 24H, CH2, CH), 2.03–2.27 (m, 2H, CH2), 3.78 (s, 1H, CH), 4.18 (s, 1H, CH), 7.95-7.97 (t, 1H, Ar–H), 7.797-7.668 (q, 2H, Ar–H), 7.245-7.270 (t, 1H, Ar–H).

Table S1 Fluorescence lifetimes obtained with two-exponential fit of the fluorescence decay curves of the RhB alone, 10 mmol L^{-1} NaDC/10 mmol L^{-1} RhB, 20 mmol L^{-1} NaDC/10 mmol L^{-1} RhB, 50 mmol L^{-1} NaDC/10 mmol L^{-1} RhB, respectively.

Sample	τ_1/ns (%)	τ_2/ns (%)	τ_3/ns (%)	τ/ns average
RhB	0.1906(55.46)	0.6794(30.24)	2.2332(14.31)	0.630728
10 mmol L^{-1} NaDC/10 mmol L^{-1} RhB	0.22(67.59)	0.78(23.51)	2.77(8.89)	0.5783
20 mmol L^{-1} NaDC/10 mmol L^{-1} RhB	0.7091(74.32)	3.0839(25.68)		1.318948
50 mmol L^{-1} NaDC/10 mmol L^{-1} RhB	0.9784(49.65)	3.4939(50.35)		2.24495